Depth profile study of ferroelectric $PbZr_{0.2}Ti_{0.8}O_3$ films

Y. Li, V. Nagarajan, S. Aggarwal, R. Ramesh, L. G. Salamanca-Riba, and L. J. Martínez-Miranda[a)]
Department of Materials and Nuclear Engineering, University of Maryland and Materials Research Science and Engineering Center, College Park, Maryland 20742-2115

(Received 15 April 2002; accepted 19 August 2002)

We have performed depth profile studies of the structure of $PbZr_{0.2}Ti_{0.8}O_3$ films of different thicknesses deposited on $SrTiO_3$ substrates prepared by pulsed laser deposition, using grazing incident x-ray scattering (GIXS). The in-plane structure of the films reveals these consist of up to three domains, one *c*-axis domain, and two *a*-axis domains, denoted $a1$ and $a2$. GIXS measurements show the evolution of in-plane compression of the lattice parameter as a function of depth within the films, particularly in the $a1$ domains. This strain evolution is accompanied by the presence of twist grain boundaries in the plane in some films. The measured in-plane lattice parameters are asymmetric, which suggests an orthorhombic distortion of the lattice in the plane of the films. © *2002 American Institute of Physics.* [DOI: 10.1063/1.1513195]

I. INTRODUCTION

The lattice mismatch and thermally induced stresses between a substrate and a ferroelectric film can radically change the dielectric, ferroelectric, and electromechanical properties of the ferroelectric film. When the thickness of the films exceeds a certain value (h_{cr}), the system relieves the induced stresses through polydomain formation. A tetragonal lattice, with edges equal to *c* (the longest) and *a*, will subdivide itself into different polydomains where *c* or *a* alternate being normal to the substrate's surface. This polydomain structure is a result of minimization of the elastic energy, with three variants, $c/a_1/c/a_1$, $c/a_2/c/a_2$, and $a_1/a_2/a_1/a_2$, where *c* is the longest edge of the tetragonal unit cell and a_1 and a_2 are the edges of the cube face;[1–3] a_1 and a_2 are close to the edge *a*, but vary depending on their interaction with the substrate.

Work on $PbZr_{0.2}Ti_{0.8}O_3$ (PZT) films deposited on $SrTiO_3$ (STO) have shown that the average out-of-plane lattice parameter in *c*-domain films varies as a function of film thickness.[4,5] The average tetragonality of the films decreases and approaches bulk values with increasing thickness, with a corresponding decrease in the measured spontaneous polarization of the films.[6] In these films, the polydomains mentioned above are not uniform through the thickness of the films, but exhibit a V-shape domain wall, associated with the compressive strain due to the lattice mismatch between PZT and STO. This result suggests the presence of a distribution of lattice parameters within the films. The presence of such distribution may affect the dielectric response of the films, which in turn limits the range of thicknesses that may be used in a specific application.[6]

We have studied the structural evolution in PZT films grown on STO with a thin $La_{0.5}Sr_{0.5}CoO_3$ (LSCO) bottom electrode by pulsed laser deposition, using grazing incidence x-ray diffraction (GIXS). This method allows us to measure the in-plane structure as a function of depth in PZT films nondestructively. By performing a mapping of the in-plane scattering profile, we have observed the presence and evolution of a strain distribution in the films in the plane of the film, as a function of depth within the film, and also as a function of film thickness.

Our results suggest the *a* and *c* domains have different lattice parameters in the plane, and indicate the presence of two types of *a* domains within the films, designated $a1$ and $a2$. The $a1$ domains exhibit a *c*-axis compression as a function of depth within the films. This compression is not uniform in the plane of the film. In addition, thick films exhibit an in-plane azimuthal angle dependence, which suggests the presence of twist grain boundaries along the normal to the films, primarily close to the surface of the films.

II. EXPERIMENT

We have studied samples of PZT deposited on (001) STO substrates with 500 Å LSCO electrode, in a thickness range between 600 and 3000 Å. The samples were deposited at 650 °C in 100 mTorr oxygen partial pressure, using pulsed laser deposition.[5] The bulk lattice parameters at 25 °C for PZT, STO, and LSCO are shown in Table I. At room temperature, bulk PZT has a tetragonal unit cell with a lattice mismatch of 0.5% and 5% for the *a* and *c* axis, respectively, with STO.

The grazing incidence x-ray scattering (GIXS) technique, illustrated in Fig. 1, combines the principle of total external reflection, sample absorption, and diffraction to probe different depths within a film.[7–9] With appropriate x-ray energies, regions close to the buried film-substrate interface can also be probed.[10] By rocking the sample about the azimuthal angle ϕ, the in-plane evolution of the lattice parameters can be determined, as well as the scattering distribution about the main peaks. The GIXS experiments were performed at the National Synchrotron Light Source at Brookhaven National Laboratories, at beamlines X18A, using 1.307 Å, and 1.190 Å x rays, with a wave vector resolu-

a)Author to whom all correspondence should be addressed; electronic mail: martinez@eng.umd.edu

 © 2002 American Institute of Physics

Downloaded 28 Oct 2005 to 134.79.34.54. Redistribution subject to AIP license or copyright, see http://jap.aip.org/jap/copyright.jsp

TABLE I. Bulk room temperature lattice parameters for $PbZr_{0.2}Ti_{0.8}O_3$ (PZT), $SrTiO_3$ (STO), and $La_{0.5}Sr_{0.5}CoO_3$ (LSCO) at room temperature.

Compound	Bulk lattice constants at room temperature	
	a (Å)	c (Å)
$PbZr_{0.2}Ti_{0.8}O_3$	3.935	4.135
$SrTiO_3$	3.905	
$La_{0.5}Sr_{0.5}CoO_3$	3.83	

tion of $\Delta q = 0.002 q_O$ Å^{-1}. The x-ray beam had a spot size of 2×1 mm^2. The beam has a horizontal convergence of 6 mrad and a vertical convergence of 1.2 mrad. Diffraction is done with the detector moving in the vertical plane. Depth within the films was controlled by varying the incidence angle of the beam between 0° and 0.6°, using a Huber goniometer head with an angular step resolution of 0.025°. The error in the penetration depth is mostly due to the error in the angular step. In moving from an angle α_1 to another angle $\alpha_1 + \Delta\alpha$, all depths from 0 to α_1 and from 0 to $\alpha_1 + \Delta\alpha$ are integrated exponentially.

The depth within the films was calibrated by a measurement of the critical angle of the films obtained from the reflectivity curve for the films.[7–10] This latter measurement was performed before the in-plane measurements and served to align the surface of the film with respect to the x-ray beam. The measured critical angle was lower than the expected value based on the bulk density of PZT. These measurements indicated that the density of the films was 7.34 g/cm^3, or about 94% of the bulk density of 7.8 g/cm^3. This lower density can be caused by a variety of parameters, including the presence of pinholes and vacancies in the films. Hence the penetration length within the films is larger than expected. The reduced density results in a decrease the linear absorption coefficient μ of the films. This variation in this quantity is more difficult to determine. The depths measured using GIXS varied between 30 and 1800 Å. Measurements taken at angles corresponding to depths exceeding the thickness of the films contain information of the entire films plus the substrate background.

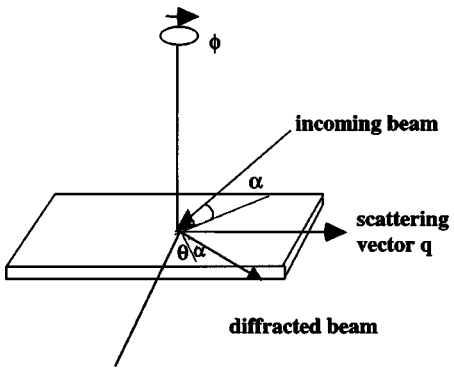

FIG. 1. Geometry of the GIXS technique: a is the x-ray beam incidence angle, **q** is the in-plane scattering wave vector, and ϕ is the azimuthal rocking angle.

III. RESULTS AND DISCUSSION

Figures 2 and 3 show the results of in-plane azimuthal scans at different incidence angles obtained in PZT films grown on LSCO/STO substrates. These two-dimensional scans are obtained by combining a number of diffraction scans (2θ) at specific azimuthal angles ϕ. The corresponding depths are shown on each panel. The films' thicknesses are 1000 and 3000 Å, respectively. The measurements were taken at 1.191 Å for the 1000 Å sample, and 1.307 Å for the 3000 Å sample. We show the {200} region for both samples. Figures 2 and 3 show the presence of *a* and *c* domains in the plane of the sample. The 3000-Å-thick sample exhibits two clearly distinguishable peaks, whereas the 1000 Å sample, except at the surface, consists of a main peak and a tail which extends to smaller angles (larger lattice parameters). The 1000 Å film has a very small peak at higher angle (not shown), which is close to the LSCO lattice parameter of 3.83 Å. This peak represents $<4\%$ of the film, and it may correspond to a small quantity of LSCO that mixes with the sample when it is deposited. It is unlikely to be a strained portion of the PZT since this represents a 2.6% compression for the short edge (a), which is large.

Figure 4 shows the evolution of the in-plane lattice parameters for the 3000, 1000, and 600 Å films as a function of depth within the film. The values have been plotted in the same scale to emphasize the differences between the samples. All films consist of a number of in-plane domains, corresponding to pairings of axes 90° apart in the plane, including the thinner 600 Å film. Previously, the presence of domains in the 600 Å films had not been observed.[6] These domains are not uniform through the thickness of the films. In the following description, we denote the domains by their corresponding out-of-plane terms: for example, a *c*-axis domain corresponds to a domain where the *c* or long axis of the PZT unit cell lies along the normal to the film.

The first domain consists of two in-plane axes with values close to the PZT *a* axis and the STO lattice parameters. These correspond to the *c* domains and can be seen in Fig. 4(a), *a* at $\phi = 180° - 181°$, and *a* at $\phi = 269° - 271°$; in Fig. 4(b), *a* and *a*1 at $\phi = 0°$ and *a* at $\phi = 90°$, and in Fig. 4(c), *a* at $\phi = 0°$ and $\phi = 90°$. The in-plane cross sectional area for this domain remains almost constant through the thickness of the films on all films as can be seen in Table II.

A second domain consists of a lattice parameter close to the PZT *a* axis and a longer axis that evolves as a function of depth in the film. The in-plane cross sectional area for this domain decreases as a function of depth in the film as we see in Table II. These correspond to *c* at 179°–180° and *a* at 269°–271° for the 3000 Å film; and *cshoul* at 0° and *a* at 90° for the 1000 Å. We note that we cannot distinguish whether the *a* axis belongs to the *c* or *a* domain. For the 1000 Å film, this cross section near the bottom of the film is close to that of the *c* domains described above. The trend toward a smaller in-plane cross section is also present in the 3000 Å film. Further reduction in the cross section is not observed because depth measurements on the 3000 Å film are limited to the first half of the film only. The observed compressive stress is coupled to the azimuthal rotation as the depth in-

Downloaded 28 Oct 2005 to 134.79.34.54. Redistribution subject to AIP license or copyright, see http://jap.aip.org/jap/copyright.jsp

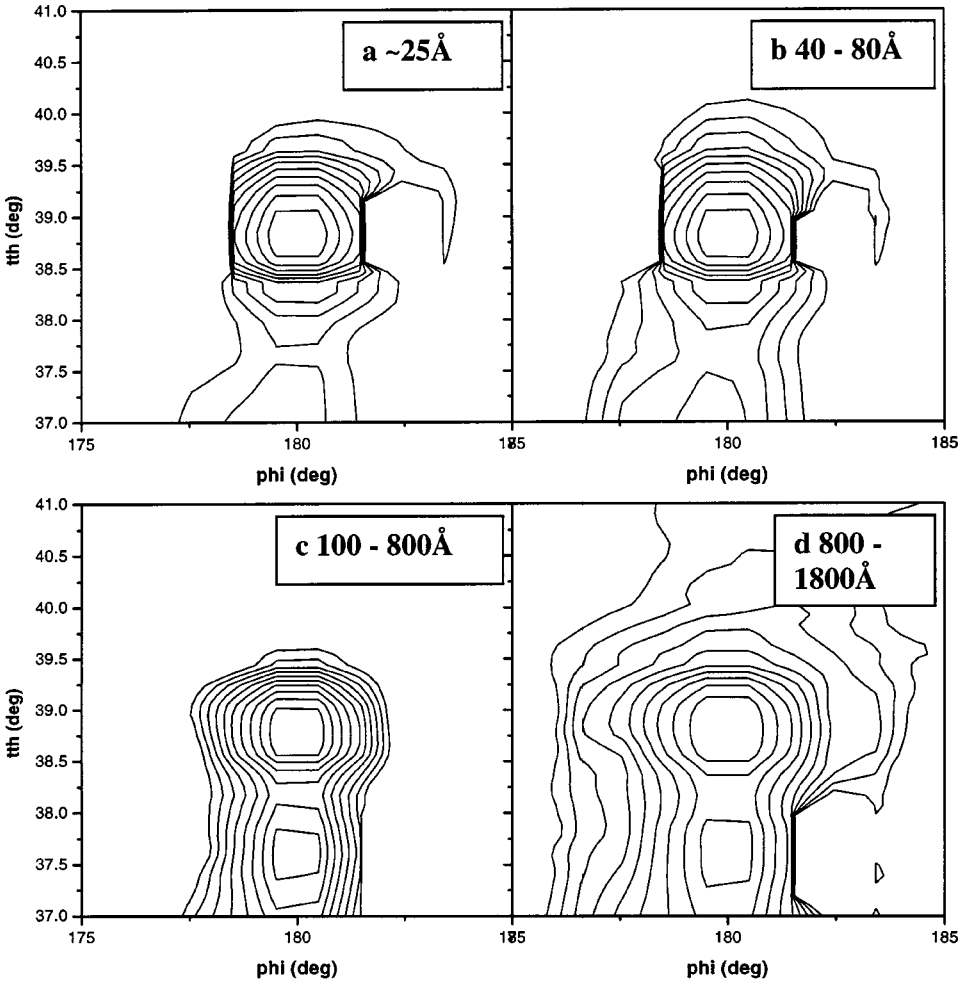

FIG. 2. Two-dimensional contour mapping of the in-plane diffraction peaks of a 3000-Å-thick film, at various depths within the film. The penetration depths are shown in the upper right corner of each panel. The diffraction peaks rotate with respect to each other as a function of depth. The sample was measured using 1.307 Å x rays.

creases, illustrated in Fig. 2. We note that the lattice compression continues after the two regions line up along the azimuth of the film. These domains correspond to *a*-axis domains near the surface of the film and transform into *c*-axis domains as the interface is approached, probably by the development of defects in the films. Figures 3 and 4(b) for the 1000 Å film show that relaxation of the lattice parameters begins within the first 200–300 Å above the interface of the film. This number agrees closely with the theoretically estimated value of 100 Å for the critical thickness of the films.[1,2] Figure 4(c) shows that this domain is not present in the 600 Å film.

A third domain observed consists of two dissimilar lattice parameters whose values vary as a function of the thickness of the film. These are the regions *c* at 271° and *a* at 179°–181° in the 3000 Å film [Fig. 4(a)]; *c* (designated by $c1$ to distinguish it from *cshoul* in Fig. 4(b)] at 90° and *a* at 0° in the 1000 Å film [Fig. 4(b)]; and the *c* at 0° and *a* at 90° in the 600 Å film [Fig. 4(c)]. The long axis for this domain represents a 1% compression of the PZT bulk *c* axis in the 3000 and 1000 Å films, respectively, coupled to a short axis which is close to the PZT bulk value. The value of the long axis parameter varies through the thickness of the 1000 Å film, as can be seen in Fig. 4(b). The short axis for the 600 Å film is close in value to the lattice parameter of the STO substrate, corresponding to a 0.6% compression. The value of the long axis is constant throughout this film. Its value of 4.15 Å constitutes a 0.3% expansion of the bulk *c*-axis parameter for PZT. This latter domain also corresponds to an *a*-axis domain, which we will denote by $a2$. The value of the in-plane unit cell cross section for this domain does not vary significantly as a function of depth in the 600 and 3000 Å films, and varies slowly for the 1000 Å film. The average value for the long (*c*-axis) lattice parameters of this domain in the 1000- and 3000-Å-thick films is close to the average value between the room temperature lattice parameter of 4.135 Å and the estimated lattice parameter 1 °C below the Curie temperature of 4.023 Å.[5] A comparison with the bulk *a*-axis parameters in this temperature range, 3.935 and 3.977 Å and Figs. 4(a) and 4(b), indicates that for this domain, the *c* axis expands by a similar amount as the *a* axis contracts.

Finally, a fourth domain can consist of a unit cell cross section made up of two long *c*-like axes in the plane of the film. However, thermodynamic models as well as previous observations indicate that this domain is not favored energetically.[1,2] The films can be viewed as consisting of three physically consistent domains, one *c* and two *a* domains, $a1$ and $a2$, one which evolves as a function of depth $(a1)$, one which remains fairly constant through the film $(a2)$.

Table II shows the values of the corresponding unit cell cross sections for the domains described above, using the

Downloaded 28 Oct 2005 to 134.79.34.54. Redistribution subject to AIP license or copyright, see http://jap.aip.org/jap/copyright.jsp

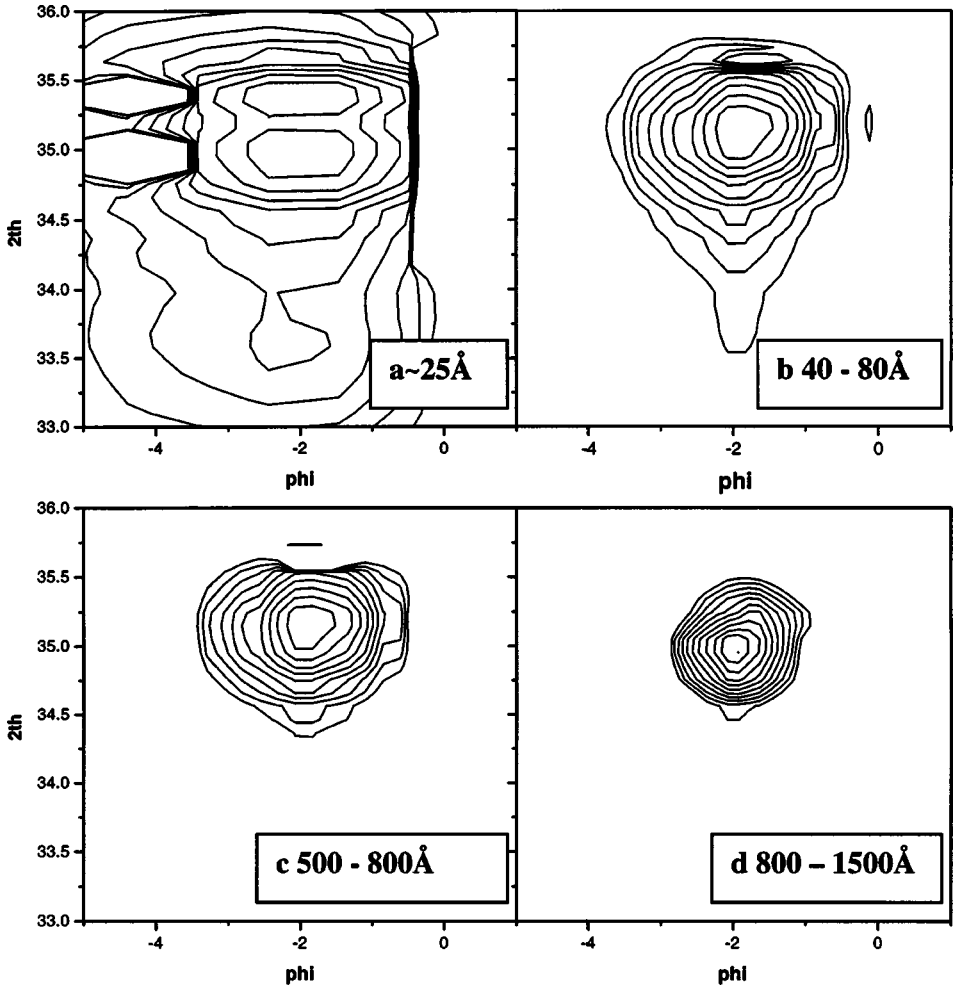

FIG. 3. Two-dimensional contour mapping of the in-plane diffraction peaks of a 1000-Å-thick film, at various depths within the film. The penetration depths are shown in the lower right corner of each panel. The sample was measured using 1.191 Å x rays.

values in Fig. 4. The above discussion indicates that the lattice evolution is asymmetric with respect to the equivalent in-plane axes in the plane of the films, and results in an orthorhombic distortion of the unit cell of the films. The observed compression in the *a* domains above is consistent with the fan-like structure exhibited by the 90° domains in PZT/STO films, observed using transmission electron microscopy (TEM).[5] The twin lines associated with the domains join close to the interface as the *c* axis contracts[1,2] and the particular in-plane direction becomes more *c*-axis oriented and more pseudomorphic with the STO substrate. This structure is not expected to exist in films close to the critical thickness value,[1,2] where the *c* axis is expected to lie entirely along the normal to the substrate. Hence the absence of such an evolution in the 600 Å films. However, the 600 Å film does show the presence of domains, but these do not exhibit an evolution with depth in the film. The evolution of the different domain structure is not directly affected by miscuts or steps in the substrate surface. In the case of STO, no apparent miscut was observed either by TEM[5] or by x ray. In the case of an $LaAlO_3$ (LAO), large optically visible miscuts were observed, but the results for the structures of the domains[10,11] were the same. The only difference was the lattice parameter of the substrate, which is closer to that of PZT for the STO substrate.

We have noted that it is very difficult to associate the *a* lattice parameter as belonging to the *c* domain or to the *a* domain. This makes it difficult to put exact numbers on the ratio of the *a* domains to *c* domains, based on the relative intensities of the peaks. It is somewhat easier for the direction where the peak is changing values (see Fig. 3 for the 1000 Å sample), because the peak only shows at a particular depth. In that case we can say that the *a* domain is disappearing in favor of the *c* domain, but we can still not assign a number since the *a* parameter can belong to the *a* domain or to the *c* domain.

We note from Table II that the measured cross section for all domains is below the expected value for the bulk tetragonal lattice in all films, which implies all films are subjected to in-plane strain. The presence of three types of domains in the 3000 and 1000 Å films leads to a distribution of lattice parameter values within the films. This is particularly the case for the $a1$ domains in the 1000 and 3000 Å films, which exhibit the largest change as a function of depth within the films, and the $a2$ domain in the 1000 Å film. According to Table II, the 1000 Å film lies in an intermediate regime between the 600 Å film and the 3000 Å film. Like the 600 Å film, it exhibits a strained *c*-domain structure. However, this structure in the 1000 Å film subdivides into two regions in the center of the film. The corresponding cross

Downloaded 28 Oct 2005 to 134.79.34.54. Redistribution subject to AIP license or copyright, see http://jap.aip.org/jap/copyright.jsp

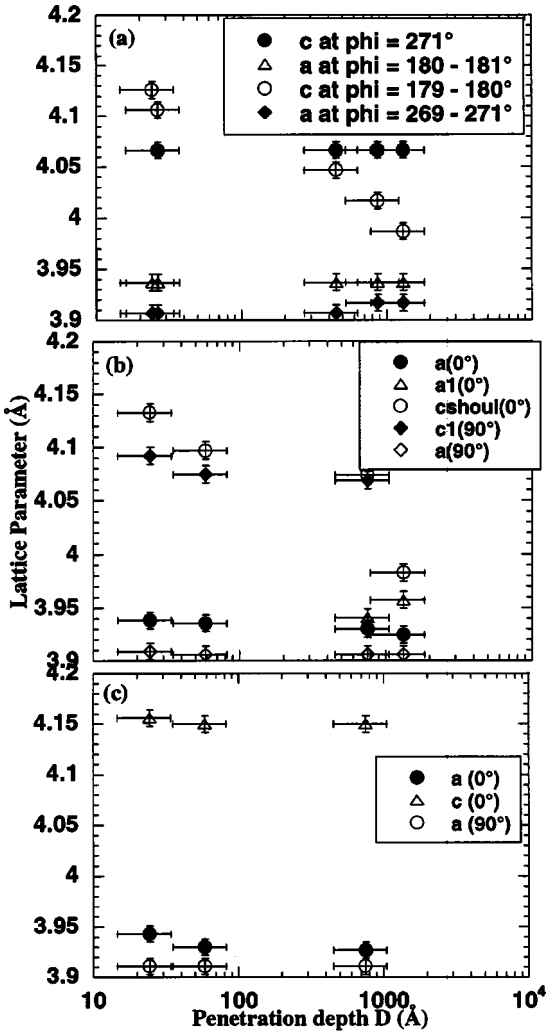

FIG. 4. Measured in-plane lattice parameters for the films presented in the text: (a) 3000-Å-thick film; (b) 1000-Å-thick film; (c) 600-Å-thick film.

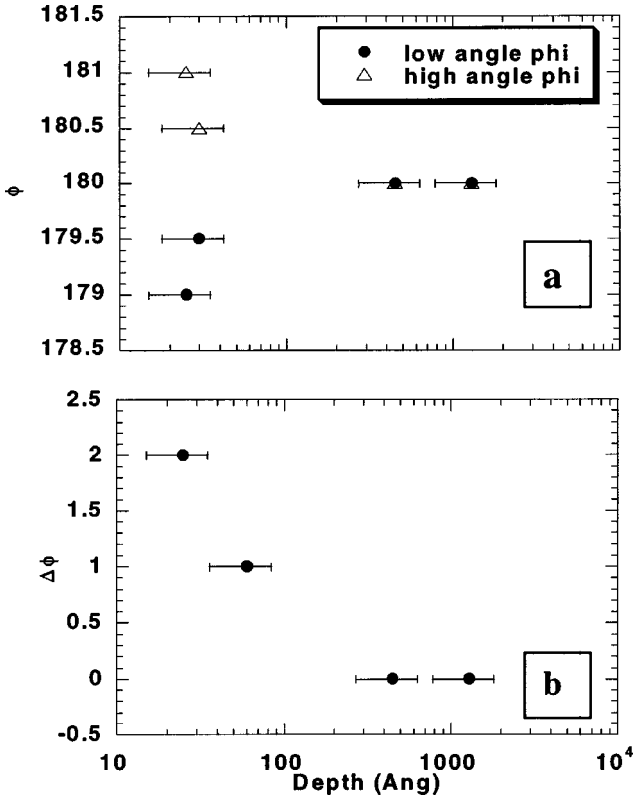

FIG. 5. In-plane lattice rotation as a function of depth: (a) Location of the peaks as depth is increased in the 3000 Å sample; (b) Difference in the azimuthal angle for the same sample in (a).

sectional area is larger for this second region, indicating the onset of relaxation within the film.

We now discuss further the process of in-plane lattice rotation. We show in Fig. 5 the evolution of the separation in azimuthal angle, $\Delta\phi$, as a function of depth for the 3000 Å film. The angle between the domains near the surface of the 3000 Å film is approximately 2°, a value close to but smaller

TABLE II. In-plane unit cell cross sectional area for the *c*, *a*1, and *a*2 domains for films 3000, 1000, and 600 Å thick. Information is taken from Fig. 4.

Thickness	Depth (Å)	*c* domain (Å^2)	*a*2 domain (Å^2)	*a*1 domain (Å^2)
600 Å				
	25	15.42	16.25	
	58	15.37	16.23	
	600	15.36	16.23	
1000 Å				
	25	15.40	16.15	16.12
	60	15.37	16.00	16.04
	750	15.35,15.39[a]	15.91	15.99
	1000	15.33,15.46[b]		15.56,15.46[b]
3000 Å				
	25	15.38		16.12
	40	15.38	16.01	16.04
	450	15.38	16.01	15.81
	800	15.42	16.01	15.73
	1800	15.42	16.01	15.62
Bulk cross sections		15.48	16.27	···

[a]Double peak.
[b]Double peak can be ascribed to either the *c* or *a* domains.

Downloaded 28 Oct 2005 to 134.79.34.54. Redistribution subject to AIP license or copyright, see http://jap.aip.org/jap/copyright.jsp

than the estimated value for the tilt value of the *a* axis with respect to the *c* axis about the normal to the film.[5,6] One possible explanation for the presence of this angle is the tetragonality of the film. As the value of the *c* axis decreases, the tetragonality decreases, resulting in a decrease of the tilt angle. The in-plane rotation suggests the presence of screw dislocations in the films, associated with the lattice relaxation through the thickness of the films. The axis rotation is independent of the substrate used, and has been observed in 2500 Å films of PZT grown on $LaAlO_3$.[10,11] However, a more detailed study of PZT films grown on LAO, indicates that lattice rotation does not occur on all films in the same thickness range, and is probably also associated with the deposition conditions.[10]

IV. CONCLUSION

We have observed the structural evolution of the in-plane lattice parameters of PZT films grown on LSCO/STO substrates. Films consist of up to three domains, observed in the plane, one *c* axis and two *a* axis. The in-plane *c* axis in one *a*1 domain undergoes a compression as a function of depth within the films. This domain transforms into a *c* domain within 200 Å of the interface, which is consistent with the calculated value of the critical thickness for these films. This compression may be coupled to a rotation of the *a* and *c* axes with respect to each other. This latter result suggests the presence of twist grain boundaries in the samples. The *c*-axis compression is consistent with the fan-shaped structure in 90° domains observed using TEM. As a consequence of the lattice evolution in the films, macroscopic properties such as the permanent polarization of the films can be the result of the superposition of the different out-of-plane *c* axes present through the film.

ACKNOWLEDGMENTS

This work was supported by NSF MRSEC Grant No. DMR-96-32521. Work at the National Synchrotron Light Source is partially supported by the U.S. Department of Energy (DOE), Contract No. DE-AC02-908CH19886. Y. Li worked on the samples to partially complete her requirements for the Master of Science at the University of Maryland.

[1] A. L. Roytburd, J. Appl. Phys. **83**, 228 (1998).
[2] A. L. Roytburg, J. Appl. Phys. **83**, 239 (1998).
[3] S. P. Alpay and A. L. Roytburg, J. Appl. Phys. **83**, 4714 (1998).
[4] B. S. Kwak, A. Erbil, J. D. Budai, M. F. Chihsolm, L. A. Boatner, and B. J. Wilkens, Phys. Rev. B **49**, 14865 (1994).
[5] S. P. Alpay, V. Nagarajan, L. A. Bendersky, M. D. Vaudin, S. Aggarwal, R. Ramesh, and A. L. Roytburg, J. Appl. Phys. **85**, 3271 (1999).
[6] S. Nagarajan, I. G. Jenkins, S. P. Alpay, H. Li, S. Aggarwal, L. Salamanca-Riba, A. L. Roytburd, and R. Ramesh, J. Appl. Phys. **86**, 595 (1999).
[7] See, for example, W. C. Marra, P. Eisenberger, and A. Y. Cho, J. Appl. Phys. **50**, 6927 (1979); M. F. Toney, T. P. Russell, J. A. Logan, H. Kikuchi, J. M. Sands, and K. Kumar, Nature (London) **374**, 709 (1995); M. F. Toney, T. C. Huang, S. Brennan, and Z. Rek, J. Mater. Res. **3**, 351 (1988).
[8] T. C. Huang and B. R. York, Appl. Phys. Lett. **50**, 389 (1987); M. F. Doerner and S. Brennan, J. Appl. Phys. **63**, 126 (1988).
[9] L. J. Martínez-Miranda, Y. Hu, and T. K. Misra, Mol. Cryst. Liq. Cryst. **329**, 121 (1999).
[10] M. Petit, V. Nagarajan, S. Aggarwal, R. Ramesh, and L. J. Martínez-Miranda, Integr. Ferroelectr. **29**, 127 (1999).
[11] Y. Li, A. Dhote, S. Aggarwal, R. Ramesh, and L. J. Martínez-Miranda (unpublished).

Downloaded 28 Oct 2005 to 134.79.34.54. Redistribution subject to AIP license or copyright, see http://jap.aip.org/jap/copyright.jsp